Journal of Sound and Vibration (1999) **224**(3), 395–410
Article No. jsvi.1998.2191, available online at http://www.idealibrary.com on IDEAL®

THE EFFECT OF WALL JOINT ON THE VIBRATIONAL POWER FLOW PROPAGATION IN A FLUID-FILLED SHELL

M. B. Xu, X. M. Zhang and W. H. Zhang

Department of Naval Architecture and Ocean Engineering, Huazhong University of Science and Technology, 430074 *Wuhan, Hubei, People's Republic of China*

(*Received* 3 *September*, 1997 *and in final form* 24 *November* 1998)

A fluid-filled cylindrical shell comprising a wall joint is investigated by using the concept of vibrational power flow. The power flow in the contained fluid and in the shell wall of this fluid-filled elastic cylindrical shell is studied. The transmission loss of vibrational power flow through the wall joint is studied and an analysis of power flow transmission and reflection at the joint in fluid-filled shells is presented. Material stiffness of the joint and frequency are two important factors that are found to strongly influence the results. It is hoped that the analysis will shed some light on the control of vibrational propagation in shells filled with fluid.

1. INTRODUCTION

Piping systems conveying fluid are used widely in many defense and industrial applications. Besides transmitting useful quantities, piping systems often transmit unwanted energy in the form of structural and acoustical vibrations. Because it can reflect a part of the incident wave and thus reduce the amplitude of the transmitted vibration, the wall joint is commonly used to control noise and vibration in practical engineering applications. In recent years, the concept of vibrational power flow has been widely used to evaluate the capacity of some isolating devices because it combines both the force and the velocity at the same time. Hence it is a fundamental topic to predict the influence of the wall joint on vibrational power flow transmission.

Discontinuities of various forms have been studied by many previous authors. Wave propagation in shells with a wall joint has been studied by Harari [1]. The discontinuity considered consists of a spring-type rubber insert and the results obtained show high power reflection coefficients at the cut-on frequencies of various torsional waves. Harari [2] has also investigated the related problem of travelling waves encountering a ring stiffener attached to the shell wall. Fuller [3] has investigated the effects of discontinuities in the wall of a cylindrical shell *in vacuo* on travelling flexural waves. Xu *et al.* [4] studied not only the amplitude, but also the angle of the reflection coefficient.

Due to the coupling between the structure and the fluid, it is much more difficult to investigate fluid-filled shells. During recent years, a lot of attention has been paid to coupled fluid-shell systems. Fuller and Fahy [5] performed an analysis

0022-460X/99/280395 + 16 $30.00/0

of dispersion curves and energy distributions between the shell and the contained fluid for a single-mode travelling with circumferential modal number $n = 0$, 1 in a fluid-filled elastic pipe. The problem of mechanical excitation of the shell wall has also been considered in a paper by Fuller [6], in which the input mobility and energy distributions in a fluid-filled infinite cylindrical shell were evaluated for line and point-driving forces applied to the shell wall. The propagation of vibrational waves through wall discontinuities in a water-filled shell has been considered by Xu *et al.* [7]. The results were also compared with those of a shell *in vacuo*.

In this paper, an analysis of wave transmission and reflection at the wall joint in fluid-filled shells is presented. Because reflection of the wall joint is the main reason for reducing wave propagation in this article, the damping of the joint material is ignored. The power transmission is used to evaluate the role of the joint. The results in this paper provide theoretical guidance on reducing noise and vibration in piping systems conveying fluid.

2. FREE WAVE PROPAGATION OF THIS COUPLED SYSTEMS

The co-ordinate system and the modal shapes are shown in Figure 1. The vibrational motion of the shell can be described by the Flügge shell equations as

$$u_{xx} + \frac{1+\mu}{2}u_{x\theta} + \frac{1-\mu}{2}v_{x\theta} + \mu w_x + K\left[\frac{1-\mu}{2}u_{x\theta} - w_{xxx} + \frac{1-\mu}{2}w_{x\theta\theta}\right]$$

$$- \rho R^2(1-\mu^2)/Eu_{tt} = 0, \tag{1a}$$

$$\frac{1+\mu}{2}u_{x\theta} + v_{\theta\theta} + \frac{1-\mu}{2}v_{xx} + w_\theta + K\left[\frac{3(1-\mu)}{2}v_{xx} - \frac{3-\mu}{2}w_{xx\theta}\right]$$

$$- \rho R^2(1-\mu^2)/Ev_{tt} = 0, \tag{1b}$$

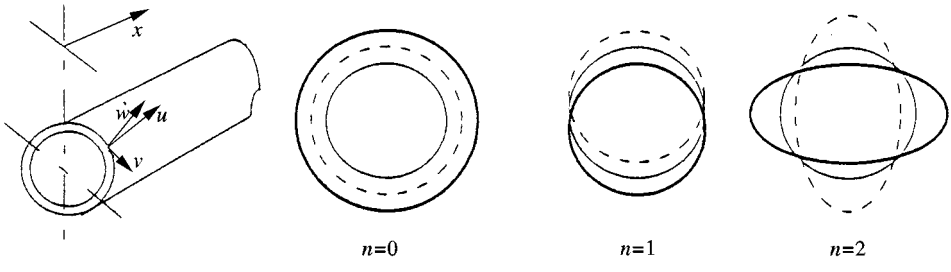

Figure 1. Co-ordinate system and modal shapes.

$$K\left[\frac{1-\mu}{2}u_{x\theta\theta} - u_{xxx} - \frac{3-\mu}{2}v_{xx\theta} + w_{xxxx} + 2w_{xx\theta\theta} + w_{\theta\theta\theta\theta} + 2w_{\theta\theta} + w\right]$$

$$+ \mu u_x + v_\theta + w + \rho R^2(1-\mu^2)/Ew_{tt} = p_f R^2(1-\mu^2)/(Eh). \tag{1c}$$

In these equations, u, v and w are shell displacements in the x, θ and r directions, respectively, R is the shell mean radius, h is the shell thickness, μ is the Poisson ratio, ρ is the density of the shell material, E is the Young's modulus, $()_x = R(\partial()/\partial x)$, $()_\theta = \partial()/\partial\theta$, $()_t = \partial()/\partial t$, K is the thickness factor, $K = h^2/12R^2$, p_f is the pressure of the contained fluid.

The solutions of equation (1), in discrete form, can be expresed as

$$u(x,\theta) = \sum_{n=0}^{\infty} u(x)\cos(n\theta) = \sum_{s=1}^{\infty}\sum_{n=0}^{\infty} U_{ns}\cos(n\theta)\exp(\mathrm{i}\omega t + k_{ns}x),$$

$$v(x,\theta) = \sum_{n=0}^{\infty} v(x)\sin(n\theta) = \sum_{s=1}^{\infty}\sum_{n=0}^{\infty} V_{ns}\sin(n\theta)\exp(\mathrm{i}\omega t + k_{ns}x), \tag{2}$$

$$w(x,\theta) = \sum_{n=0}^{\infty} w(x)\cos(n\theta) = \sum_{s=1}^{\infty}\sum_{n=0}^{\infty} W_{ns}\cos(n\theta)\exp(\mathrm{i}\omega t + k_{ns}x).$$

The associated form of the pressured field in the contained fluid, which satisfies the acoustic wave equation, is given as

$$p(x,\theta) = \sum_{n=0}^{\infty} p(x)\cos(n\theta) = \sum_{s=1}^{\infty}\sum_{n=0}^{\infty} P_{ns}\cos(n\theta)\,J_n(k_s^r r)\exp(\mathrm{i}\omega t + k_{ns}x), \tag{3}$$

when n is the circumferential modal number, s denotes a particular branch of the dispersion curves, ω is the driving frequency, $J_n()$ is Bessel function of order n. k_{ns} and k_s^r are the axial and radial wavenumbers, respectively. The radial wavenumber k_s^r is related to the axial wavenumber k_{ns} by the usual vector relation $(k_s^r R)^2 = \Omega^2(C_L/C_f)^2 - (k_{ns}R)^2$, where Ω is the non-dimensional frequency, and C_L and C_f are the wave speed in the shell and in the fluid, respectively.

Application of the fluid momentum equation at the shell wall, $r = R$, results in

$$P_{ns} = [\omega^2\rho_f/k_s^r J_n'(k_s^r R)]\,W_{ns}, \tag{4}$$

where ρ_f is the density of the contained fluid and the prime denotes differentiation with respect to the argument $k_s^r R$.

Substitution of equations (2)–(4) into the shell equations (1) results in the equations of motion of the coupled system in symmetric matrix form:

$$[L_{3\times 3}][U_{ns}\ \ V_{ns}\ \ W_{ns}]^T = [0\ \ 0\ \ 0]^T, \tag{5}$$

$$\begin{bmatrix} \lambda^2 + a' & b'\lambda & c'\lambda^3 + d'\lambda \\ & e'\lambda^2 + f' & g'\lambda^2 + h' \\ & & j' + k'\lambda^2 + l'\lambda^4 - FL \end{bmatrix} \begin{bmatrix} U_{ns} \\ V_{ns} \\ W_{ns} \end{bmatrix} = \begin{bmatrix} 0 \\ 0 \\ 0 \end{bmatrix}, \tag{6}$$

$$\lambda = k_{ns}R,\ a' = -(1-\mu)(1+K)n^2/2 + \Omega^2,\quad b' = (1+\mu)n/2,\quad c' = -K,$$

$$d' = \mu - K(1-\mu)n^2/2,\quad e' = -(1-\mu)(1+3K)/2,\quad f' = n^2 - \Omega^2,$$

$$g' = -(3-\mu)Kn/2,\quad h' = n,\quad j' = 1 + K(n^2-1)^2 - \Omega^2,\quad k' = -2n^2K, \tag{7}$$

$$l' = K,\quad \Omega^2 = \rho_s R^2\omega^2(1-\mu^2)/E,$$

where FL is the fluid loading term due to the presence of the fluid acoustic field and is given by

$$FL = \Omega^2(\rho_f/\rho_s)(h/R)^{-1}(k_s^r R)^{-1}[J_n(k_s^r R)/J_n'(k_s^r R)]. \tag{8}$$

Expansion of the determinant of the amplitude coefficient in equation (5) provides the system characteristic equation

$$P_1(\lambda) - P_2(\lambda)FL = 0, \tag{9}$$

where both $P_1(\lambda)$ and $P_2(\lambda)$ are polynomial. For the sake of brevity, the coefficients are not given here.

Due to the "non-linearity" of the equation, numerical methods have to be employed to find the desired eigenvalues. The eigenvalues will be either pure real, pure imaginary or complex. The pure real and imaginary roots can be found by the method of bisection. Newton's downhill method and the plane grille searching method are combined to find the complex roots. For each circumferential modal number n, these wavenumbers λ can be separated into two groups. The first group contains backward waves associated with a semi-infinite shell, $-\infty < x < 0$ (left side), excited at the edge at $x = 0$. The second group describes forward waves associated with a semi-infinite shell, $0 < x < \infty$ (right side), excited at the edge at $x = 0$. If λ is pure real or pure imaginary, one obtains a near-field wave or a propagating wave, respectively. If λ is complex is conjugate pairs, one obtains an atenuated standing wave, which means that the wave amplitudes decay in one direction but the waves propagate in both directions.

By substituting the roots back into equation (5), the characteristic vectors are obtained as

$$\begin{cases} \phi_{0s} = \dfrac{U_{0s}}{W_{0s}} \\ \varphi_{0s} = 0 \end{cases} \quad \textit{for } n = 0,$$

$$\begin{cases} \phi_{ns} = \dfrac{U_{ns}}{W_{ns}} = \dfrac{L_{12}L_{23} - L_{13}L_{22}}{L_{11}L_{22} - L_{12}L_{21}} \\ \varphi_{ns} = \dfrac{V_{ns}}{W_{ns}} = \dfrac{L_{21}L_{13} - L_{11}L_{23}}{L_{11}L_{22} - L_{12}L_{21}} \end{cases} \quad \text{for } n > 0. \tag{10}$$

As $n = 0$, the torsional mode of the shell is uncoupled from all other motions and has been omitted. Φ_{ns} and Ψ_{ns} characterize the particular type of wave motion, giving the ratio of longitudinal and circumferential displacements to the flexural displacement.

3. POWER FLOW IN THIS COUPLED SYSTEM

When waves propagate through this fluid-filled shell, there will be vibrational power flow in the shell wall and the contained fluid.

3.1. POWER FLOW IN THE CONTAINED FLUID

The fluid field can be described by the usual pressure solution in cylindrical coordinates for a particular circumferential mode n as

$$p = \sum_{s=1}^{S} P_{ns} \cos(n\theta) J_n(k_s^r r) \exp(\mathrm{i}\omega t + k_{ns} x), \tag{11}$$

where S is the total number of propagating waves.

The axial acoustic particle velocity can be obtained from the momentum relation

$$v_x = \frac{-1}{\mathrm{i}\rho_f \omega} \frac{\partial p}{\partial x}. \tag{12}$$

Thus the axial velocity is

$$v_x = \sum_{s=1}^{S} \frac{k_{ns}}{\rho_f \omega} P_{ns} \cos(n\theta) J_n(k_s^r r) \exp(\mathrm{i}\omega t + k_{ns} x). \tag{13}$$

Acoustic power intensity in the axial direction is expressed as

$$I(\theta, r, t) = \frac{1}{2} \operatorname{Re} al(p v_x^*) = \sum_{s=1}^{S} \frac{P_{ns}}{2} \frac{k_{ns}}{\rho_f \omega} \cos^2(n\theta) J_n^2(k_s^r r), \tag{14}$$

where * denotes the complex conjugate.

Then the total power flow in the contained fluid P_{fluid} is obtained by integrating the power intensity given by equation (14) flowing through an element of area

$\mathrm{d}A = \mathrm{r}\,\mathrm{d}\theta\,\mathrm{d}r$ over the cross-sectional area of the fluid field. The power flow P_{fluid} is

$$P_{fluid} = \int_0^{2\pi}\int_0^R I(\theta, r, t)\,\mathrm{d}A = \sum_{s=1}^{S}\int_0^{2\pi}\int_0^R \frac{P_{ns}^2}{2}\frac{k_{ns}}{\rho_f\omega}\cos^2(n\theta)J_n^2(k_s^r r)r\,\mathrm{d}\theta\,\mathrm{d}r \quad (15)$$

$$= \frac{\eta_n\pi}{2\rho_f\omega}\sum_{s=1}^{S} P_{ns}^2 k_{ns}\int_0^R J_n^2(k_s^r r)r\,\mathrm{d}r, \quad (16)$$

where $\eta_n = 2$ when $n = 0$, and $\eta_n = 1$ when $n > 0$.

As discussed in section 2, by application of the boundary condition at the shell wall, the power in the contained fluid can be written in terms of the shell radial amplitude W_{ns}. Substituting equation (4) into equation (16) result in

$$P_{fluid} = \frac{\eta_n\pi\rho_f\omega^3}{2}\sum_{s=1}^{S} W_{ns}^2 k_{ns}[k_s^r J_n'(k_s^r R)]^{-2}\int_0^R J_n^2(k_s^r r)\,r\,\mathrm{d}r. \quad (17)$$

The integral in equation (17) takes the form of Lommel's integral, the solution of which can be written as [8]

$$\int_0^R J_n^2(k_s^r r)r\,\mathrm{d}r = 0{\cdot}5R^2\left\{[J_n'(k_s^r R)]^2 + \left(1 - \frac{n^2}{(k_s^r R)^2}\right)J_n^2(k_s^r R)\right\}. \quad (18)$$

Then the power flow in the contained fluid can be obtained easily.

3.2. POWER FLOW IN THE SHELL WALL

When there are propagating waves in this fluid–shell system, there will exist four forces of the cylindrical shell section in the axial direction. These forces for a particular circumferential mode n can easily be derived from the exact Flügge shell equations as

$$N_x = \sum_{s=1}^{S} N_{ns}W_{ns}\cos(n\theta)\mathrm{e}^{k_{ns}x + \mathrm{i}\omega t},$$

$$T_x = \sum_{s=1}^{S} T_{ns}W_{ns}\sin(n\theta)\mathrm{e}^{k_{ns}x + \mathrm{i}\omega t},$$

$$S_x = \sum_{s=1}^{S} S_{ns}W_{ns}\cos(n\theta)\mathrm{e}^{k_{ns}x + \mathrm{i}\omega t}, \quad (19)$$

$$M_x = \sum_{s=1}^{S} M_{ns}W_{ns}\sin(n\theta)\mathrm{e}^{k_{ns}x + \mathrm{i}\omega t},$$

where W_{ns} is the amplitude of the flexural displacement, N_x, T_x, S_x and M_x are the axial force, torsional shear force, transverse shear force and bending moment in the x direction, respectively, and can be written as

$$N_{ns} = \frac{D}{R}\,[\phi_{ns}\lambda_{ns} + \mu n\varphi_{ns} + \mu - K\lambda_{ns}^2],$$

$$T_{ns} = \frac{D}{R}\,\frac{(1-\mu)}{2}\,[-n\phi_{ns} + (1+3K)\varphi_{ns}\lambda_{ns} + 3Kn\lambda_{ns}],$$

$$S_{ns} = \frac{D}{R}\,K[(\lambda_{ns}^3 - \mu n^2\lambda_{ns} - \phi_{ns}\lambda_{ns}^2 - \mu n\varphi_{ns}\lambda_{ns})$$

$$-(1-\mu)(2n^2\lambda_{ns} + \tfrac{1}{2}n^2\phi_{ns} + \tfrac{3}{2}n\varphi_{ns}\lambda_{ns})],$$

$$M_{ns} = DK[\lambda_{ns}^2 - \mu n^2 - \phi_{ns}\lambda_{ns} - \mu n\varphi_{ns}],$$

$$K = \frac{h^2}{12R^2}, \quad D = \frac{Eh}{(1-\mu^2)}.$$

The power flows in the shell wall at the section, transmitted by these forces, are given as

$$\begin{aligned} P_{nx} &= 0{\cdot}5\eta_n\pi\ \mathrm{Re}[\mathrm{i}\omega N_x u^*], \\ P_{tx} &= 0{\cdot}5\eta_n\pi\ \mathrm{Re}[\mathrm{i}\omega T_x v^*], \\ P_{sx} &= 0{\cdot}5\eta_n\pi\ \mathrm{Re}[\mathrm{i}\omega S_x w^*], \\ P_{mx} &= 0{\cdot}5\eta_n\pi\ \mathrm{Re}\left[\mathrm{i}\omega M_x \frac{\partial w^*}{\partial x}\right]. \end{aligned} \tag{20}$$

Then the total power in the shell wall is

$$P_{shell} = P_{nx} + P_{tx} + P_{sx} + P_{mx}. \tag{21}$$

3.3. TOTAL POWER FLOW IN THE COUPLED SYSTEM

When waves propagate through this coupled system, the total power flow is the sum of the power both in the shell and in the contained fluid. Then,

$$P_{total} = P_{shell} + P_{fluid}. \tag{22}$$

4. THE EFFECT OF WALL JOINT ON THE POWER PROPAGATION

The shell conveying fluid with a wall joint is shown in Figure 2. The material of the shell is steel, the wall joint is made of hard rubber, and the fluid is water. When there is an incident propagating wave in region (a), the joint will reflect some power carried by the incident wave, and thus the power carried by the transmitted wave in region (c) is less than the incident power in region (a) and the vibration can be reduced. All local effects of a discontinuity in wall thickness such as local stress concentrations are ignored. This approximation is justified by the initial assumption that the wall thickness is very small compared to the shell radius and the thickness parameter is retained only in flexural terms of the characteristic equation.

The discontinuity is to be analyzed by dividing the shell into sections as in Figure 2 and considering wave propagation and reflection in each. The wave incident on the joint is assumed to be a propagating wave $s = 1$ for various values of circumferential mode n. Theoretically, a single incident wave of mode order n will generate infinite reflected waves or (and) transmitted waves in regions (a)–(c) with an identical mode order. The boundary conditions (BC) at each discontinuity in the wall of the shell will include the continuity of angular bending velocity, radial, axial and tangential velocity, and the continuity of angular bending moment, transverse shear, axial force and torsional shear. In the *fluid*, BC will include the continuity of pressure p and axial velocity v_x at every point of the interfaces A and B. Thus the number of BC will be infinite in theory and *cannot be* satisfied in reality.

To the vibration waves, only the lower order types will be considered. That is, all the propagating waves and attenuated standing waves will be included. As for the near-field waves, only those with small wavenumbers will be included.

The BC in the shell wall and the mean value of p and v_x in the *contained fluid* will be included first. The continuity of p and v_x at some points of the interface A and B (for example $r = 0$, $r = 0{\cdot}5R$) will also be included as boundary conditions. Then the problem will arise as to how many waves and BC have to be considered on earth. When an incident propagating wave is reflected by the joint, the vibrational power flow carried by the incident wave will convey into the power flow carried by the reflected and transmitted waves. Moreover, the incident power will be equal to

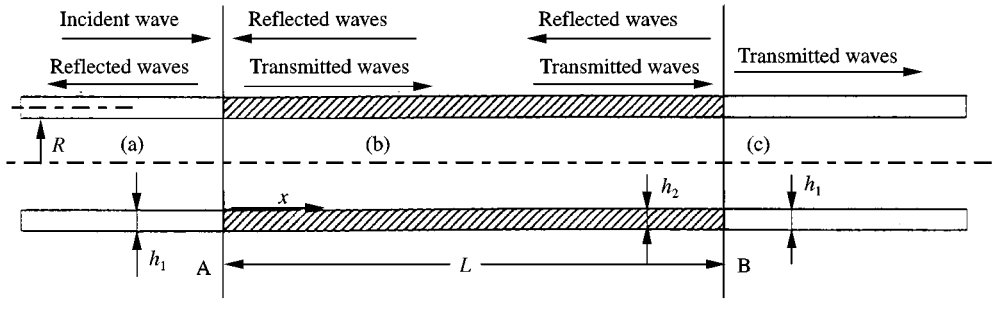

Figure 2. Arrangement of the wall joint.

the sum of the reflected and the transmitted power. According to the principle of energy conversation, we can decide the number of waves and BC.

At interfaces A and B, for example, the continuity of radial velocity of the shell wall provides an equation

$$\left(- W_{nl}^{ia} + \sum_{s=1}^{S} W_{ns}^{ra} \right)\Bigg|_{A:x=0} = \left(- \sum_{s=1}^{S} W_{ns}^{tb} + \sum_{s=1}^{S} W_{ns}^{rb} \right)\Bigg|_{A:x=0}, \tag{23}$$

$$\left(\sum_{s=1}^{S} W_{ns}^{tb} - \sum_{s=1}^{S} W_{ns}^{rb} \right)\Bigg|_{B:x=1} = \left(\sum_{s=1}^{S} W_{ns}^{tc} \right)\Bigg|_{B:x=1}, \tag{24}$$

where the amplitude of the incident wave is assumed to be unity and S is the total number of considered waves; superscripts a, b and c refer to the corresponding sections shown in Figure 2; i, r and t refer to the incident wave, reflected waves and transmitted waves, respectively.

Similarly, by applying other boundary conditions at both interfaces A and B, other equations can be provided and an equation group containing $4 \times S$ equations will be obtained. The $4 \times S$ unknown complex coefficients of the $4 \times S$ equations were set into a $4S \times 4S$ matrix and the unknown Fourier amplitudes were then evaluated. Thus the main amplitude of each considered wave was obtained.

Then the power flows carried by the incident wave, transmitted waves and reflected waves can be calculated. The vibrational power flow carried by the reflected and the transmitted waves is defined as

$$P^r = \sum_{s=1}^{S} P_{total}^{ra}, \tag{25}$$

$$P^t = \sum_{s=1}^{S} P_{total}^{tc}, \tag{26}$$

The power carried by the incident wave is

$$P^i = P_{total}^{ia}. \tag{27}$$

If the difference between $P^t + P^r$ and P^i is small, the results will be correct; if otherwise, more waves and BC have to be considered until the difference is small. In engineering, the frequency of the wave cannot be too high, and hence it is unnecessary to consider too many waves and BC.

The power transmission is used to investigate the effect of the wall joint and is defined as

$$Tr = P^t/P^i. \tag{28}$$

5. RESULTS AND DISCUSSIONS

A shell conveying fluid with a wall joint is considered. The incident vibration wave is assumed to be the first propagating wave $s = 1$. The material of the shell is stell. The parameters of the shell are: the poisson ratio $\mu = 0{\cdot}3$, Density $\rho_s = 7800\ \text{kg/m}^3$, Young's modulus $E = 1{\cdot}92 \times 10^{11}\ \text{N/m}^2$, mean radius $R = 0{\cdot}1$ m, thickness $h/R = 0{\cdot}05$, the wave speed in the shell $C_L = 5200$ m/s. The contained fluid is water, the wave speed $C_f = 1500$ m/s, and the density $\rho_f = 1000\ \text{kg/}m^3$. Several kinds of wall joints, with variations of Young's modulus E, thickness h_2/R and length L/R, are investigated. The parameters of these wall joints are given in Table 1.

The results and discussion about the dispersion curves of a fluid-filled shell had been given in reference [5] and not given here for the sake of brevity. Hence only the effect of the wall joint on the power flow transmission is given in this part.

5.1. THE EFFECT OF $n = 0$ ON THE TORSIONAL WAVE

When $n = 0$, torsional motion is uncoupled, and so the effect on the shell filled with water will be the same as that of a shell *in vacuo*. See reference [4].

5.2. THE EFFECT OF $n = 0$ ON THE COUPLED WAVES

5.2.1. The power transmission with variations of Young's modulus E of the joint

In order to evaluate the influence of Young's modulus E on the power flow propagation, a shell with joint A, B or C is studied. The results of power transmission are plotted in Figure 3.

Some conclusions can be drawn. No matter what value Young's modulus E of the joint is, $Tr = f(\omega)$ is a periodic function, which means that the Tr will decrease and increase periodically with an increase in frequency ω. When frequency ω is very low, the joint hardly reflects the incident propagating wave and thus the power flow can transmit without loss, that is, $Tr \approx 1{\cdot}0$ in the frequency region. But with an increase in frequency ω, Tr will decrease rapidly, which means that the wall joint

TABLE 1
Parameters of the wall joints

Joint	E(N/m^2)	h_2/R	L/R	ρ(kg/m^3)	μ
Joint A	$2{\cdot}0 \times 10^9$	0·05	2·0	1100·0	0·4
Joint B	$4{\cdot}0 \times 10^9$	0·05	2·0	1100·0	0·4
Joint C	$1{\cdot}0 \times 10^9$	0·05	2·0	1100·0	0·4
Joint D	$2{\cdot}0 \times 10^9$	0·1	2·0	1100·0	0·4
Joint E	$2{\cdot}0 \times 10^9$	0·025	2·0	1100·0	0·4
Joint F	$2{\cdot}0 \times 10^9$	0·005	1·0	1100·0	0·4
Joint G	$2{\cdot}0 \times 10^9$	0·005	4·0	1100·0	0·4

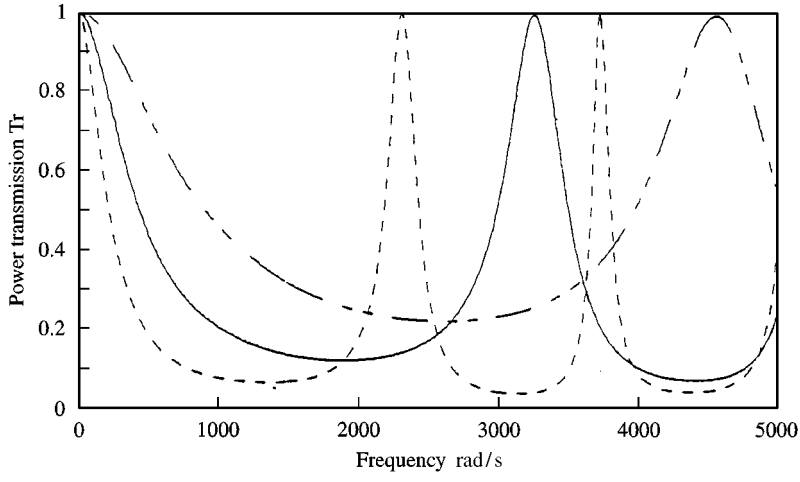

Figure 3. Power transmission Tr with variation of the Young's modulus of the joint. E. $n = 0$ ——— Joint A; — – – — Joint B: – – – – Joint C.

plays a more important role in reducing the incident vibration. This can be explained by the following reasons. The assumed incident wave $s = 1$ is a fluid-type wave in low frequency, the vibrational energy of which is contained mainly in the fluid and the fluid-filled shell vibrates in dominantly fluid motion. Thus the wall joint (structural discontinuity) hardly reflects this incident propagating wave in this frequency region. With the increase in frequency, the vibrational energy of the incident wave $s = 1$ will be contained both in the fluid and in the shell wall. Thus the wall joint will reflect the incident wave and Tr will decrease rapidly. By comparing different values of Young's modulus E, it can be found that with a decrease in Young's modulus E, the period of function $Tr = f(\omega)$ will decrease and the mean value of Tr will decrease also. This can be explained by the relative stiffness of the shell and the wall joint. As the Young's modulus E of the wall joint decreases, the stiffness difference between the shell and the joint will increase. Thus the wall joint will reflect the incident power more effectively and Tr will decrease too.

5.2.2. The power transmission with variations of the thickness h_2/R of the joint

The results of joints with different values of joint thickness are plotted in Figure 4. It can be concluded that the effect of the thickness h_2/R on the Tr is similar to that of the Young's modulus E. For the sake of brevity, the results are not discussed further. By comparing Figure 4 with Figure 3, It can be seen that the results of joints B and C are almost the same as those of joints D and E, respectively.

This can be explained by the definition of membrane stiffness D. Since $D = Eh/(1 - \mu^2)$,

$$E_{Joint-B} = 4{\cdot}0 \times 10^9, \quad \frac{h_{Joint-B}}{R} = 0{\cdot}05, \quad E_{Joint-C} = 1{\cdot}0 \times 10^9, \quad \frac{h_{Joint-C}}{R} = 0{\cdot}05,$$

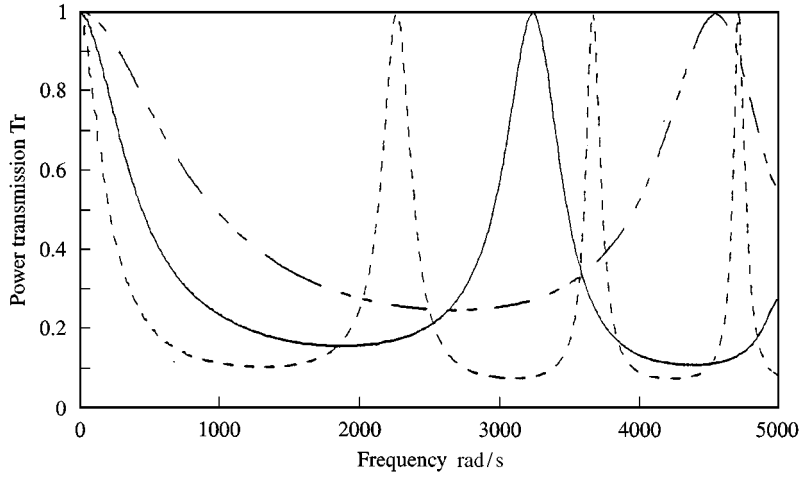

Figure 4. Power transmission Tr with variation of joint thickness h. $n = 0$. ———— Joint A; — – – – Joint D; – – – – Joint E.

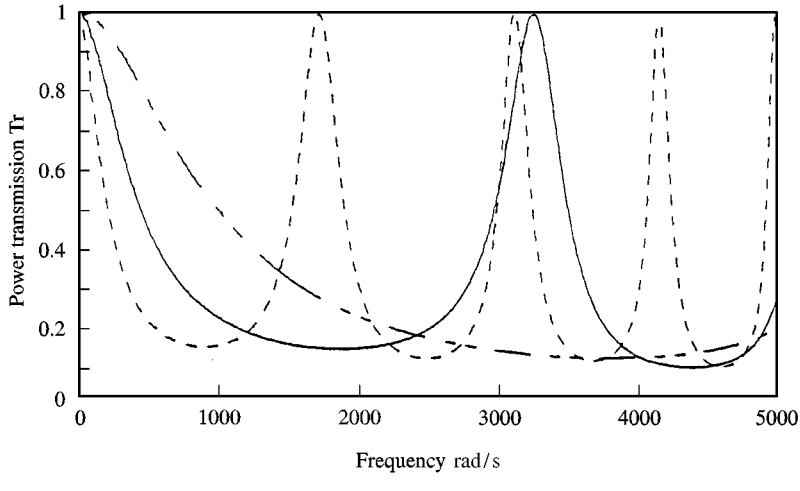

Figure 5. Power transmission Tr with variation of joint length L. $n = 0$. ———— Joint A; — – – – Joint F; – – – – Joint G.

$$E_{Joint-D} = 2{\cdot}0 \times 10^9, \quad \frac{h_{Joint-D}}{R} = 0{\cdot}1, \quad E_{Joint-E} = 2{\cdot}0 \times 10^9, \quad \frac{h_{Joint-E}}{R} = 0{\cdot}025,$$

so $D_{Joint-B} = D_{Joint-D}$ and $D_{Joint-C} = D_{Joint-E}$, the results of Joint B and C are almost the same as those of joints D and E, respectively.

5.2.3. The power transmission with variations of length L/R of the joint

The results with variations of length L/R are given in Figure 5. $Tr = f(\omega)$ is also a periodic function. By comparing the results of joints A, F and G, it can be seen

that the period of the function $Tr = f(\omega)$ will double if the length L/R of the joint decreases from 2·0 to 1·0, and period will be half if the length L/R increases from 2·0 to 4·0. This means a longer joint should be chosen if the driving frequency region is wide.

5.3. THE EFFECT OF $n > 0$ ON THE COUPLED WAVES

When $n = 1$, in order to study the effect of Young's modulus E, thickness h_2/R and length L/R, the power transmission of joints A, B, C, D, E, F and G are plotted in Figures 6–8. The results are similar to those of $n = 0$ and thus not discussed further for the sake of brevity.

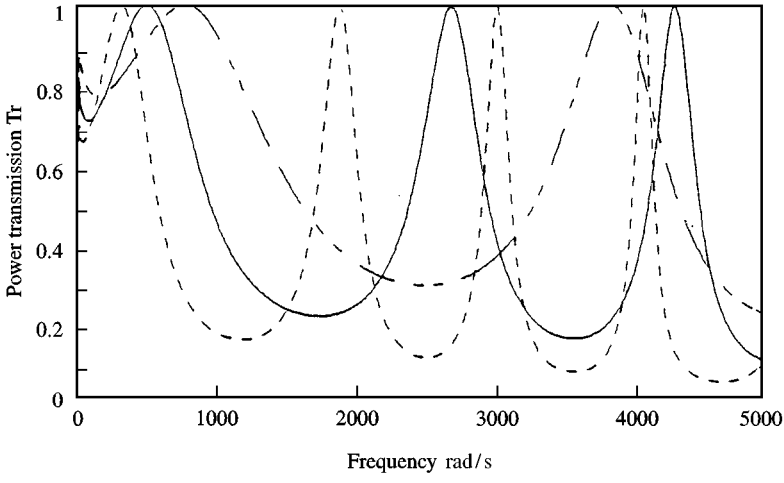

Figure 6. Power transmission Tr with variation of the Young's modulus of the joint. E. $n = 1$ ———— Joint A; — – – — Joint B: – – – – Joint C.

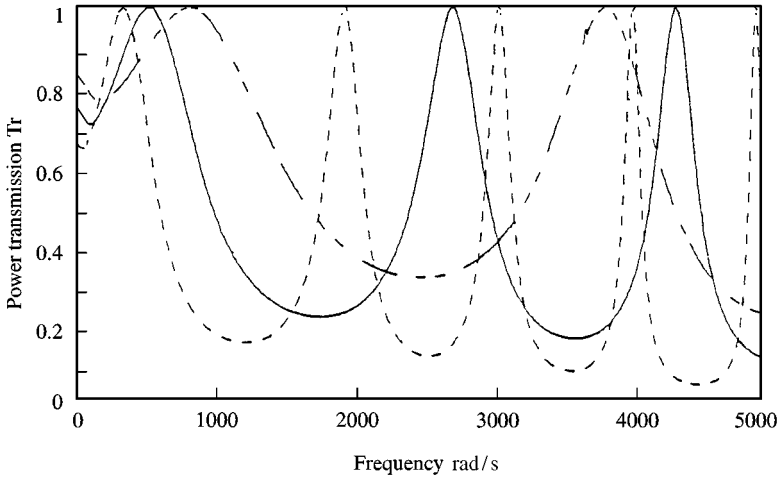

Figure 7. Power transmission Tr with variation of joint thickness h. $n = 1$. ———— Joint A; — – – — Joint D; – – – – Joint E.

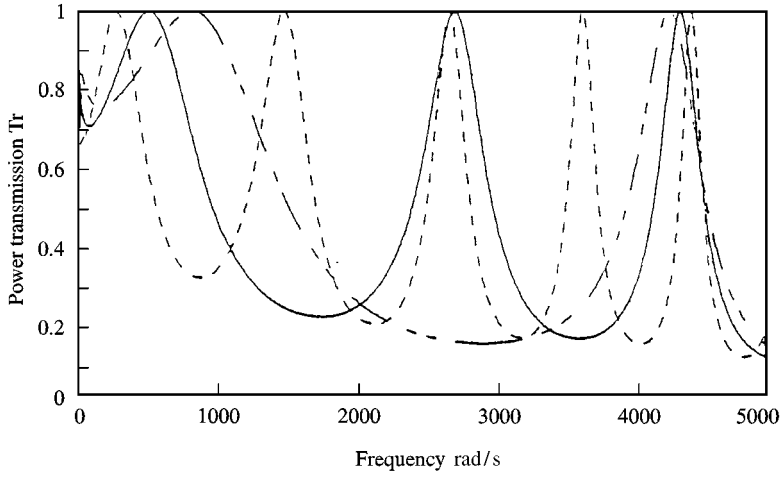

Figure 8. Power transmission Tr with variation of joint length L. $n = 1$. ———— Joint A; — – – — Joint F; – – – – Joint G.

However, an evident difference exists between $n = 0$ and $n > 0$ when the driving frequency is very low. For the breathing mode $n = 0$, the wall joint hardly reflects the incident propagating wave and thus $Tr = 1{\cdot}0$ in this frequency region; for other modes ($n > 0$), the wall joint reflects the incident propagating wave and thus $Tr < 1{\cdot}0$ in the same region. This difference is due to the characteristics of the incident propagating wave. For the breathing mode $n = 0$, there are two propagating waves at low frequencies; the energy of the first wave $s = 1$ is contained in the fluid, while the energy of the second wave $s = 2$ is concentrated in the shell wall. In the analysis, the incident wave is assumed to be the first wave $s = 1$, and thus the joint in the shell wall hardly reflects the incident wave $s = 1$ and $Tr = 1{\cdot}0$ in this frequency region. For the modes $n > 0$, the incident propagating wave $s = 1$ is largely in the form of shell wall vibration, and so the wall joint plays an important role in the controlling of the incident vibration propagation and $Tr < 1{\cdot}0$ in the same region.

6. CONCLUSIONS

The power transmission associated with the incident vibrational wave $s = 1$ impinging on various joints in the wall of a fluid–filled cylindrical shell has been studied. From the above discussion, a conclusion can be drawn that the geometry and physical parameters of the wall joint have significant effects on the vibrational power flow transmission and reflection in a fluid-filled shell. When the *difference of parameters* between the joint and the shell increases, the effect of the wall joint on vibrational isolation will be more effective.

ACKNOWLEDGEMENT

The authors are grateful for the financial assistance provided by the National Natural Science Foundation of China (Contract No. 19044005).

REFERENCES

1. A. HARARI 1978 *Shock and Vibration Bulletin* **48**, 53–61. Wave propagation in a cylindrical shell with joint discontinuity.
2. A. HARARI 1977 *Journal of the Acoustical Society of American* **62**, 1196–1205. Wave propagation in a cylindrical shell with finite region of structural discontinuity.
3. C. R. FULLER 1981 *Journal of Sound and Vibration* **75**, 207–228. The effect of wall discontinuities on the propagation of flexural waves in cylindrical shells.
4. M. B. XU, X. M. ZHANG and W. H. ZHANG 1996 *Journal of Huazhong University of Science and Technology* **24**, 72–75. The effect of wall joint on the power flow propagation in cylindrical shells.
5. C. R. FULLER and F. J. FAHY 1982 *Journal of Sound and Vibration* **81**, 501–518. Characteristics of wave propagation and energy distributions in cylindrical elastic shells filled with fluid.
6. C. R. FULLER 1983 *Journal of Sound and Vibration* **87**, 409–427. The input mobility of an infinite circular cylindrical elastic shell filled with fluid.
7. M. B. XU, X. M. ZHANG and W. H. ZHANG 1995 *Proceedings, International Conference on Structural Dynamics, Vibration, Noise and Control, SDVNC'95, Hong Kong*. The effect of wall discontinuities on the wave propagation in a fluid-filled elastic cylindrical shell.
8. N. W. MCLACHLAN 1934 *Bessel Functions for Engineers*. London: Oxford University Press.
9. W. FLÜGGE 1973 *Stress in Shells*. New York: Springer.

APPENDIX: NOMENCLATURE

C_f	fluid acoustic free wave speed
C_L	shell extension phase speed
D	membrane stiffness
E	Young's modulus
FL	fluid loading term
h	shell-wall thickness
i	$\sqrt{-1}$
J_n0	Bessel function of order n
k_0	free wavenumber
k_{ns}	axial wavenumber
k_s^r	radial wavenumber
L	length of the joint
M_x	bending moment of the shell wall
N_x	axial force
n	circumferential modal number
P_{fluid}	power in the contained fluid
P_{shell}	power in the shall wall
P_{total}	power in the system
P^i	power flow by the incident wave
P^r	power flow by the reflected wave
P^t	power flow by the transmitted wave
R	shell mean radius
s	branch number of the waves
S	number of the considered waves
S_x	transverse shear force
T_x	torsional shear force
Tr	power transmission
u, v, w	shell displacements

x, θ, r	cylindrical co-ordinate
ϕ, φ	characteristic vectors
ρ_f	density of fluid
ρ_s	density of shell
μ	Poisson's ratio
ω	circular frequency
Ω	non-dimension frequency
λ	non-dimension wavenumber

Superscripts

a, b, c	discontinuity sections
i, r, t	incident, reflected, transmitted
*	complex conjugate
$'$	differentiation